Mesophase Formation in Regioregular Poly(3-alkylthiophene)s Containing Long Chain Alkyl Groups

Yu Wang,[†] Nadia Archambault,[†] Allison M. Belcher,[†] Devin Busse,[†] David B. Damon,[‡] Ashley Mills,[†] Amanda E. Riddle,[†] Ivan J. Samardjiev,[‡] Brett L. Lucht,*[,†] and William B. Euler*[,†]

Department of Chemistry, 51 Lower College Road, University of Rhode Island, Kingston, Rhode Island 02881, and Pfizer Global Research and Development, Eastern Point Road, Groton, Connecticut 06340

Received June 16, 2008; Revised Manuscript Received July 29, 2008

ABSTRACT: A series of regioregular poly(3-alkylthiophene)s with substituent groups R = $C_{22}H_{45}$, $C_{24}H_{49}$, $C_{26}H_{53}$, and $C_{28}H_{57}$ were synthesized. All of the materials can form a mesophase by rapid quenching from the isotropic melt. The ease of mesophase formation depends upon the length of the alkyl group, with the longer side chains leading to mesophase formation at lower quenching rates. Variable temperature reflection and fluorescence spectroscopy of thin films and differential scanning calorimetry and variable temperature X-ray diffraction on powders were used to study the thermal behavior of the new polymers. All of the materials studied showed a two-step thermochromic transition from the mesophase, and endotherms in the thermograms could be assigned to melting of each phase. The data indicate that $\pi-\pi$ stacking is an important contributor to the thermochromism observed in these compounds while the interaction between the alkyl side chains controls mesophase formation.

Introduction

Conjugated polymers have received significant attention due to the unique combination of processability and optoelectric properties.[1] This combination of properties has resulted in the use of conjugated polymers in organic light-emitting diodes (OLEDs), field effect transistors (FETs), solar cells, and other interesting electronic applications.[2] Control of the structural features of the conjugated polymer is critical in each of these applications. Substituted poly(3-alkylthiophene)s are among the most widely investigated conjugated polymers.[3] While poly(3-alkylthiophene)s (PATs) can be doped to generate a conductive state, in their reduced form PATs are deeply colored materials that strongly absorb in the visible region. The electronic absorption spectra of many PATs are dependent upon temperature or solvent.[4] The thermochromic and solvatochromic properties of PATs have been investigated in detail to afford a thorough understanding of the electronic states of these interesting materials.[5−16]

As part of our investigation of the thermochromic and solvatochromic properties of PATs, we uncovered an unusual two-step thermochromism in poly(3-docosylthiophene).[16−18] Pristine samples prepared at room temperature are a violet color. Upon slow heating, poly(3-docosylthiophene) changes to the well-known high-temperature yellow color. When poly(3-docosylthiophene) is cooled slowly to ambient, the original violet color is reestablished. However, when poly(3-docosylthiophene) is cooled rapidly, the final color is red, distinctly different from the pristine color. The original violet color can be reestablished by heating the red sample to yellow and then slowly cooling. This process can be repeated for tens to hundreds of cycles. A well-defined endotherm in the DSC thermogram was found for each process. The red phase is stable at room temperature for long times—we have samples that have retained this phase for more than 3 years.

In this article, we have expanded our investigation of poly(3-alkylthiophene)s with very long *n*-alkyl side chains. We have synthesized the regioregular forms of poly(3-docosylthiophene) (**PDT**), poly(3-tetracosylthiophene) (**PTT**), poly(3-hexacosylthiophene) (**PHT**), and poly(3-octacosylthiophene) (**POT**). Variable temperature reflection and luminescence spectroscopies were used to characterize the thermochromic properties of the materials. Differential scanning calorimetry (DSC) was used to investigate the thermal properties. The thermochromic transition temperatures associated with the mesophase generally increase with increased length of the side chain. The rate of cooling required for generation of the mesophase decreases as the length of the side chain increases. The presence of an isolatable mesophase by rapid quenching with new thermochromic properties strongly argues that interchain phenomena (aggregation and crystallization) are critical components in understanding the mechanism of thermochromism in poly(3-alkylthiophene)s. These conclusions are supported by variable temperature X-ray diffraction (XRD) measurements reported here.

Experimental Section

Synthesis. *1-Bromotetracosane (***1***).* Under nitrogen, 1-octadecylmagnesium bromide (generated from 96 mmol of 1-bromooctadecane and 125 mmol of magnesium turnings) in 150 mL of anhydrous THF was transferred to a dry flask containing 287 mmol of 1,6-dibromohexane, 0.96 mmol of copper(I) bromide, and 50 mL of anhydrous THF under nitrogen at 0 °C. After reacting overnight at room temperature, the product was washed in a mixture of 100 mL of dilute HCl, 200 mL of diethyl ether, and 100 mL of hexanes. The organic layer was washed to neutral with water. Recrystallization in 350 mL of acetone yielded 36 g of crude product. Column chromatography over silica gel in hexanes afforded 26.5 g (67%) of the title compound. ^{1}H NMR (400 MHz, $CDCl_3$): δ 3.42 (t, 2H), 1.86 (m, 2H), 1.22 (m, 42H), 0.89 (t, 3H). ^{13}C NMR (100 MHz, $CDCl_3$): δ 34.22, 33.08, 32.16, 29.93, 29.78, 29.67, 29.60, 29.01, 28.42, 22.92, 14.34.

*1-Bromohexacosane (***2***).* **2** was prepared similarly to **1** (from 1-bromoeicosane and 1,6-dibromohexane) followed by column chromatographic elution in hexanes to afford the title compound in 60% yield. ^{1}H NMR (400 MHz, $CDCl_3$): δ 3.41 (t, 2H), 1.86 (m, 2H), 1.18 (m, 46H), 0.89 (t, 3H). ^{13}C NMR (100 MHz, $CDCl_3$):

* Corresponding authors. E-mail: blucht@chm.uri.edu; weuler@chm.uri.edu.
[†] University of Rhode Island.
[‡] Pfizer Global Research and Development.

10.1021/ma801352f CCC: $40.75
Published on Web 09/06/2008

δ 34.17, 33.09, 32.17, 29.94, 29.79, 29.68, 29.61, 29.02, 28.43, 22.92, 14.33.

*1-Bromooctacosane (***3***).* **3** was prepared similarly to **1** (from 1-bromodocosane and 1,6-dibromohexane) followed by column chromatographic elution in hexanes to afford the title compound in 52% yield. ^{1}H NMR (400 MHz, $CDCl_3$): δ 3.42 (t, 2H), 1.86 (m, 2H), 1.22 (m, 50H), 0.89 (t, 3H). ^{13}C NMR (100 MHz, $CDCl_3$): δ 34.23, 33.09, 32.16, 29.93, 29.78, 29.68, 29.60, 29.01, 28.42, 22.92, 14.34.

*3-Tetracosylthiophene (***4***).* Under nitrogen, 13 mmol of **1** and 26 mmol of magnesium ribbon in 50 mL of anhydrous diethyl ether were refluxed overnight. The Grignard reagent was then transferred under nitrogen to a dry flask containing 13 mmol of 3-bromothiophene and 0.26 mmol of Ni(dppp)Cl_2 in 15 mL of anhydrous diethyl ether at 0 °C and stirred at room temperature (rt) overnight. The reaction mixture was then washed in dilute HCl and neutral water. Chromatographic elution in hexanes afforded the title compound in 66% yield. ^{1}H NMR (400 MHz, $CDCl_3$): δ 7.24 (m, 1H), 6.94 (m, 2H), 2.64 (t, 2H) 1.64 (m, 2H), 1.22 (m, 42H), 0.90 (t, 3H). ^{13}C NMR (100 MHz, $CDCl_3$): δ 143.48, 128.49, 125.21, 119.95, 32.17, 30.80, 30.52, 29.93, 29.71, 29.58, 22.92, 14.34.

*3-Hexacosylthiophene (***5***).* Under nitrogen, 26 mmol of **2** and 32 mmol of magnesium turnings in 100 mL of anhydrous THF were refluxed overnight. The Grignard reagent was then transferred under nitrogen to a dry flask containing 52 mmol of 3-bromothiophene and 0.52 mmol of Ni(dppp)Cl_2 in 30 mL of anhydrous THF at 0 °C and was reacted at rt overnight. The product was then washed in a mixture of 100 mL of dilute HCl and 100 mL of hexanes. The organic layer was then washed to neutral with water. Column chromatography over silica gel in hexanes afforded 7.3 g (63%) of the title compound. ^{1}H NMR (400 MHz, $CDCl_3$): δ 7.25 (m, 1H), 6.94 (m, 2H), 2.64 (t, 2H), 1.63 (m, 1H), 1.28 (m, 46H), 0.90 (t, 3H). ^{13}C NMR (100 MHz, $CDCl_3$): δ 143.49, 128.50, 125.22, 119.96, 32.17, 30.80, 30.52, 29.94, 29.71, 29.60, 22.93, 14.34.

*3-Octacosylthiophene (***6***).* **6** was prepared similarly to **5** followed by chromatographic elution in hexanes to afford the title compound in 50% yield. ^{1}H NMR (400 MHz, $CDCl_3$): δ 7.25 (m, 1H), 6.95 (m, 2H), 2.63 (t, 2H), 1.63 (m, 2H), 1.28 (m, 50H), 0.89 (t, 3H). ^{13}C NMR (100 MHz, $CDCl_3$): δ 143.36, 128.52, 125.23, 119.97, 32.17, 30.89, 30.52, 29.93, 29.71, 29.60, 22.93, 14.35.

*2,5-Dibromo-3-tetracosylthiophene (***7***).* 7.1 mmol of 3-tetracosylthiophene was dissolved in 30 mL of anhydrous THF. To this was added 14.3 mmol of *N*-bromosuccinamide over a period of 5 min. The solution was allowed to stir at rt overnight. The solvent was removed in vacuo followed by precipitation of succinamide in hexanes. After filtration and removal of hexanes in vacuo, the product was recrystallized in ether−methanol, affording **7** in 79% yield. ^{1}H NMR (400 MHz, $CDCl_3$): δ 6.78 (s, 1H), 2.51 (t, 2H), 1.55 (m, 2H), 1.23 (m, 42H), 0.89 (t, 3H). ^{13}C NMR (100 MHz, $CDCl_3$): δ 143.23, 131.19, 110.52, 108.14, 32.16, 29.93, 29.80, 29.76, 29.70, 29.59, 29.32, 22.92, 14.34.

*2,5-Dibromo-3-hexacosylthiophene (***8***).* **8** was prepared similarly to **7** and obtained in 85% yield. ^{1}H NMR (400 MHz, $CDCl_3$): δ 6.78 (s, 1H), 2.51 (t, 2H), 1.54 (m, 2H), 1.27 (m, 46H), 0.89 (t, 3H). ^{13}C NMR (100 MHz, $CDCl_3$): δ 134.21, 131.19, 110.54, 108.11, 32.16, 29.93, 29.79, 29.59, 29.32, 22.92, 14.33.

*2,5-Dibromo-3-octacosylthiophene (***9***).* **9** was prepared similarly to **7** and obtained in 86% yield. ^{1}H NMR (400 MHz, $CDCl_3$): δ 6.78 (s, 1H), 2.51 (t, 2H), 1.54 (m, 2H), 1.27 (m, 50H), 0.89 (t, 3H). ^{13}C NMR (100 MHz, $CDCl_3$): δ 143.23, 131.19, 110.52, 108.15, 32.16, 29.93, 29.80, 29.76, 29.70, 29.60, 29.33, 22.92, 14.35.

*Regioregular Poly(3-tetracosylthiophene) (***PTT***).* Under a positive pressure of nitrogen, 1.6 g of 2,5-dibromo-3-tetracosylthiophene was dissolved in 70 mL of anhydrous THF. To this was added 2.2 mL of methylmagnesium bromide (1.4 M solution in 25:75 toluene/THF) followed by refluxing for 1 h. 30 mg of Ni(dppp)Cl_2 (1% mol equiv) was added, and the reaction mixture was allowed to reflux overnight. The reaction mixture was quenched with 5 mL of methanol and then concentrated to 20 mL. The polymer was then precipitated in 100 mL of methanol and Soxhlet extracted in methanol and then hexanes. The hexanes soluble fraction was reduced and dried in vacuo to afford the title polymer in 22% yield. SEC (THF vs polystyrene): M_n = 2000, PDI = 2.2. The product remaining in the thimble was recovered to afford 19% of the title polymer. SEC (THF vs polystyrene) M_n = 6100, PDI = 1.7. ^{1}H NMR (400 MHz, THF-d_8): δ 7.05 (s, 1H), 2.29 (t, 2H), 1.27 (m, 44H), 0.88 (t, 3H).

*Regioregular Poly(3-hexacosylthiophene) (***PHT***).* **PHT** was prepared similarly to **PTT** and recovered in 46% yield after Soxhlet extraction in methanol and hexanes. Molecular weight could not be determined by GPC due to poor solubility in THF. ^{1}H NMR (400 MHz, THF-d_8): δ 7.04 (s, 1H), 2.30 (t, 2H), 1.32 (m, 48H), 0.88 (t, 3H).

*Regioregular Poly(3-octacosylthiophene) (***POT***).* **POT** was prepared similarly to **PTT** and recovered in 37% yield after Soxhlet extraction in methanol and hexanes. Molecular weight could not be determined by GPC due to poor solubility in THF. ^{1}H NMR (400 MHz, THF-d_8): δ 7.05 (s, 1H), 2.32 (t, 2H), 1.29 (m, 52H), 0.90 (t, 3H).

Mesophase Poly(3-alkylthiophene)s. Mesophases of each regioregular PAT were prepared by heating the pristine regioregular polymers past their thermochromic transition temperature and then rapidly cooling (hundreds of degrees per minute). The PAT was placed in aluminum foil, the foil was heated with a heat gun for ∼5 s, and then the foil was immediately immersed in liquid nitrogen and held for ∼20 s.

Measurements. NMR spectra were recorded on a JEOL Eclipse 400 MHz NMR spectrometer using either $CDCl_3$ or THF-d_8 as solvents. Polymer molecular weights were estimated by size exclusion chromatography (Agilent Technology series 1100 HPLC; detector: differential refractometer G1362A; pump: isocratic 1310A; software: Chemstation; column: Plgel 10^3 A using THF as solvent and polystyrene standards). Reflection and emission spectra were made using an Ocean Optics spectrometer between 400 and 800 nm. Samples were prepared by spin-coating polymer solutions onto a white piece of card stock. The same card stock was used as the white reference. The samples were placed on an aluminum block and heated at ∼2 °C/min using a hot plate. The aluminum block had a hole drilled in it for a thermometer, which was thermally linked to the block using silicone grease. The temperature of the surface of the block was calibrated using naphthalene and biphenyl by monitoring the scattering change as the calibrant melted. Temperatures recorded in this manner are accurate to ±2 °C. This experimental procedure provided a convenient procedure for temperature control applicable only to the reflection geometry, so transmission measurements were not done. The excitation source for the emission measurements was at 395 nm. Differential scanning calorimetry (DSC) was run on a TA Instruments Q100 instrument. All DSC measurements were done under flowing nitrogen at 10 °C/min unless otherwise noted. Sample sizes ranged from 2 to 5 mg (massed to 0.01 mg), were sealed in aluminum pans, and equilibrated at −50 °C prior to measurements. Variable temperature X-ray powder diffraction patterns were collected for poly(3-alkylthiophene)s using a Bruker D8 diffractometer (Pfizer Inc.) equipped with a Cu radiation source, fixed slits (divergence 2.0 mm, antiscatter 1.0 mm, and receiving 1.0 mm), and a scintillation counter detector. Data were collected in the $\theta-2\theta$ goniometer configuration from a specialized PAAR TTK sample holder with internal heating thermocup at the Cu wavelength $K_{\alpha 1}$ = 1.540 56 and $K_{\alpha 2}$ = 1.544 39 (relative intensity 0.5) from 3.0° to 40.0° 2θ using a step size of 0.040° and a step time of 1.0 s. X-ray tube voltage and amperage were set at 40 kV and 40 mA, respectively. Data were collected and analyzed using Bruker DIFFRAC Plus software. Samples were prepared by placement in specialized metal PAAR TTK sample holder with internal heating thermocup. Temperature-controlled values were navigated through PAAR-TTK temperature control system from Bruker AXS.

Regioregular poly(3-alkylthiophene)s and mesophase poly(3-alkylthiophene)s had X-ray powder diffraction patterns collected at 25, 40, 45, 50, 55, 60, 65, 70, 75, 80, 85, 90, 95, 100, 105, 110,

120, 130, and 150 °C. Mesophase poly(3-alkylthiophene)s were cooled to 25 °C after data collection at 150 °C was complete, and the cooled materials were subjected to a second heating cycle, with X-ray powder diffraction patterns collected at the same temperatures as the first heating cycle.

Results and Discussion

The preparation of long chain *n*-alkyl bromides was afforded via the copper-mediated coupling of alkylmagnesium bromides with 1,6-dibromohexane in THF. The resulting long chain alkyl bromides were then converted to the Grignard reagent and coupled with 3-bromothiophene in the presence of a nickel catalyst to yield the corresponding long chain 3-alkylthiophene. Regioregular PATs were prepared via Grignard metathesis polymerization.[20]

The molecular weights of all of the polymers could not be measured because of poor solubility in THF. PATs with substituent groups R = $C_{22}H_{45}$ and R = $C_{24}H_{49}$ have sufficient solubility for SEC measurements. For R = $C_{22}H_{45}$, M_n = 35 000 (PDI = 1.9) (**PDT**), as we reported earlier.[16,21] For the new polymers described here we find M_n = 6100 (PDI = 1.7) for R = $C_{24}H_{49}$ (**PTT**). Unfortunately, the **PTT** sample did not fully dissolve in THF. For the polymers with longer side chains the molecular weight appears to be limited by the solubility of the polymer in the reaction solvent. Thus, we expect that the polymers with R = $C_{26}H_{53}$ and R = $C_{28}H_{57}$ have molecular weight comparable to or slightly lower than the R = $C_{24}H_{49}$ samples.

Poly(3-alkylthiophene)s with long chain *n*-alkyl substituents ($\geq C_{22}H_{45}$) can be readily isolated in two different phases at room temperature. The as-synthesized materials are typically violet. If these polymers are heated, they change color to a bright yellow, the well-known thermochromic transition in poly(3-alkylthiophene)s.[5−16] When the yellow material is cooled slowly, the polymer returns to the violet state. However, if the yellow phase is cooled rapidly (tens to hundreds of degrees per minute, depending upon the specific polymer), then a mesophase is formed that is red at room temperature. Examples of the reflection spectra of the three different phases are shown in Figure 1, which demonstrate that the red phase is not a simple mixture of the yellow and violet phases.

The insets in Figure 1 show the reflectivity at a single wavelength as a function of temperature. Each sample was prepared by rapidly cooling from high temperature to give a film containing predominantly the mesophase. The plots show the sharp phase transitions between each phase. The mesophase changes to the darker annealed phase at intermediate temperature, and then, at higher temperature, the sample changes to the yellow phase. The transition temperatures are found by fitting the *%R* vs *T* curves to a double-sigmoid function of the form

$$f(R) = R_0 + \frac{a_1}{1 + e^{-(T-T_1)/\Delta T_1}} + \frac{a_2}{1 + e^{-(T-T_2)/\Delta T_2}} \qquad (1)$$

where T_1 and T_2 are the transition temperatures, ΔT_1 and ΔT_2 are the widths of the transitions, a_1 and a_2 are the reflection changes through the transition, and R_0 is the baseline reflection. The transition temperatures are summarized in Table 1.

After a sample was heated and then slowly cooled, no spectroscopic evidence of the mesophase was found. Heating of the annealed samples showed a single phase transition at T_2, as demonstrated in the insets for **PDT** and **PHT** in Figure 1. The spectra of the room temperature, slowly cooled material are the same as the spectra measured at temperatures just above T_1, the phase transition associated with the loss of the mesophase.

The emission spectra are shown in Figure 2. The mesophase has an emission peak between 615 and 630 nm (depending upon the alkyl chain length) that disappears upon heating. In the annealed phase there is weak emission for **PDT** and **PTT** and no measurable emission for **PHT** and **POT**, but further heating to the high-temperature phase leads to a relatively strong emission peak centered between 600 and 615 nm. Equation 1 (substituting emission intensity for *%R*) was used to find the transitions temperatures between the different phases as measured by the luminescence. The data at a given wavelength and the fits are shown in the insets in Figure 2. The transition temperatures found from the emission spectra match those found from the reflection spectra, as shown in Table 1. Upon cooling,

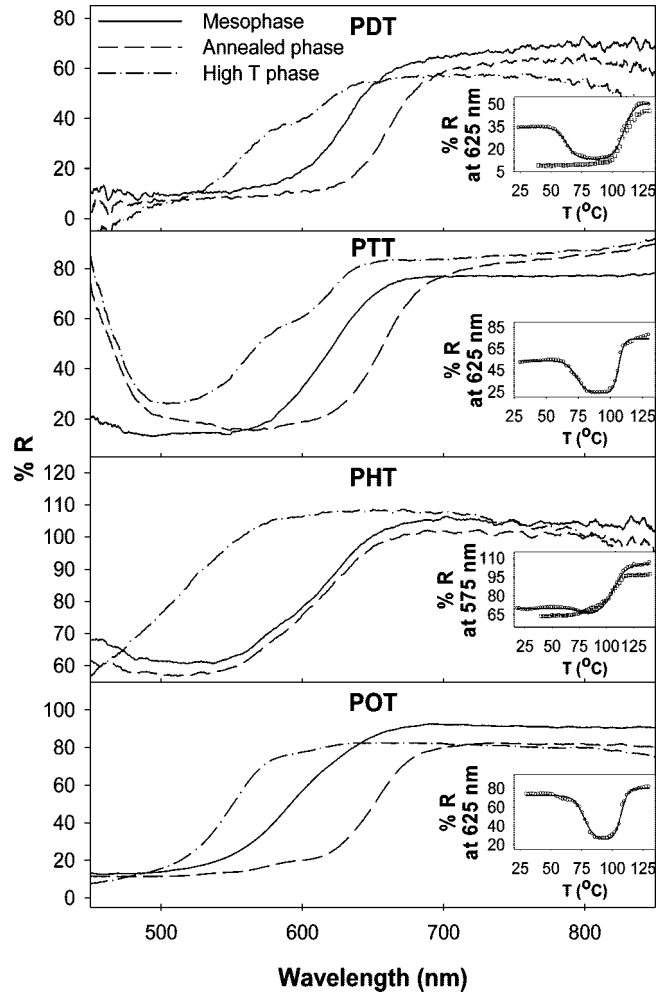

Figure 1. Reflection spectra of regioregular poly(3-alkylthiophene)s: for each sample the mesophase is shown by the black line, the annealed phase is shown by the dashed line, and the high-temperature phase is shown by the dot-dashed line. The inset for each spectrum shows the percent reflection at a single wavelength as a function of temperature for a sample starting with the mesophase: the circles are the first heating cycle, and the squares are the second heating cycle. The heating rate was about 2 °C/min. The solid line in each inset is the fit to eq 1, discussed in the text.

Table 1. Transition Temperatures (°C) Determined by Reflection and Emission Spectroscopies for Poly(3-R-thiophene)[a]

	reflection		emission	
sample	T_1	T_2	T_1	T_2
PDT	63	109	77	103
PTT	74	107	60	102
PHT	74	107	79	110
POT	77	107	75	105

[a] Multiple (2−4) samples were measured, and standard deviations were typically ∼5 °C. T_1 is the transition from the mesophase to the annealed phase, and T_2 is the transition from the annealed phase to the high-temperature phase.

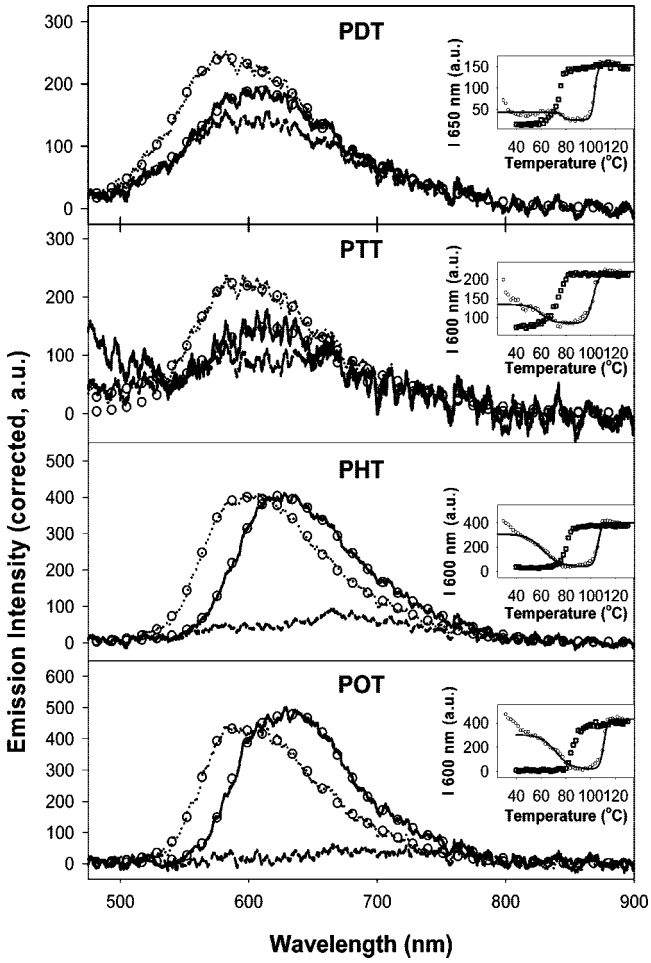

Figure 2. Emission spectra of regioregular poly(3-alkylthiophene)s using 395 nm excitation: for each sample the mesophase is shown by the black line, the annealed phase is shown by the dashed line, and the high-temperature phase is shown by the dotted line. The open circles on each spectrum are fits to multiple Gaussian functions, as discussed in text. The inset for each spectrum shows the emission intensity at a single wavelength as a function of temperature for a sample starting with the mesophase: the circles are the first heating cycle, and the squares are the second heating cycle. The heating rate was about 2 °C/min. The solid line in each inset is the fit to eq 1, discussed in the text.

there is a significant hysteresis in the loss of the emission intensity relative to the onset of the high-temperature emission. This is in contrast to the reflection spectra, where the cooling transition matched the higher temperature heating transition.

The lower temperature transition, T_1, is assigned as the loss of the mesophase, and the higher temperature transition, T_2, is assigned to the melting of the main polymer chain (vide infra). There is a small increase in T_1 as a function of increasing chain length while T_2 is constant across all samples. This suggests that the formation of the mesophase is related to the side chain structure while the transition to the high-temperature state is controlled by the polythiophene chain.

The emission spectra were deconvoluted into two to three Gaussian peaks, as demonstrated by the fits in Figure 2. The wavelength maxima found from these fits are shown in Table 2. Tachibana et al.[22] have previously reported that thin films of poly(3-alkylthiophene)s on quartz have weak exciton emission with peaks observed at 690, 750, and 830 nm, which do not match the peaks observed in the mesophase. However, at high temperatures the previous report found features at 585, 630, and 695 nm,[22] in general agreement with the results reported here.

Table 2. Wavelength Maxima Found from Deconvolution of the Emission Spectra

sample	λ (nm) mesophase	λ (nm) high-temperature phase
PDT	600, 633	565, 613, 620
PTT	601, 635, 644	576, 615, 618
PHT	608, 642, 681	574, 607, 651
POT	600, 636, 676	574, 608, 652

In agreement with the reflection spectra, the emission results imply that the mesophases have unique geometric and electronic structure. The lowest energy transitions in regioregular poly(3-alkylthiophene)s are assigned as exciton transitions originating from the conjugated π system of the polymer,[22] but there is also a contribution from the interstack $\pi-\pi$ interaction.[23] The results presented here are consistent with previous findings. The annealed phase, which has lower energy electronic transitions, must have the better conjugation along the main chain and/or stronger $\pi-\pi$ interstack interactions than the mesophase, which has a slightly blue-shifted spectrum. The high-temperature phase is strongly blue-shifted, consistent with little π-conjugation or $\pi-\pi$ interaction. The photoluminescence spectra are also consistent with these conclusions: the annealed state has weak or no measurable fluorescence because of the strong interstack interactions. The high-temperature phase has a strong emission that is blue-shifted, relative to the mesophase, and is associated with unconjugated electronic states uncoupled from the surrounding medium. The mesophase has an observable emission due to the reduced nearest-neighbor coupling but is at lower energy because some conjugation is still present along the thiophene π system.

DSC was used to probe the thermal behavior in these materials. Figure 3 shows the thermograms of the regioregular polymers that do not contain the mesophase. All of the thermograms exhibit two endotherms. The lower temperature peak is assigned to melting of the side chains, and the higher temperature feature is assigned to melting of the main polymer backbone, in accord with the literature.[10] As the length of the substituent chain increases, the side chain melting temperature also increases. In contrast, the main chain (isotropic) melting temperature is constant. The pattern in the heats of fusion are less well-defined: ΔH_{sm} (heat of fusion for the side chain melting endotherm) is generally constant with increasing side chain length while ΔH_2 (heat of fusion for the main chain melting endotherm) generally increases with increasing substituent chain

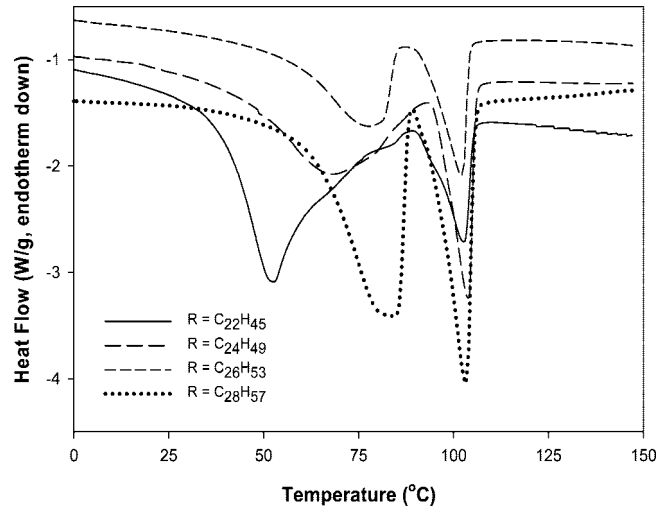

Figure 3. DSC thermograms of regioregular poly(3-alkylthiophene)s: solid line, **PDT**; long dashes, **PTT**; short dashes, **PHT**; dotted line, **POT**. All measurements are the second heating cycle so that the mesophase is removed. Scans were run at 10 °C/min under flowing nitrogen gas.

Table 3. Differential Scanning Calorimetry Results for Heating Scans[a]

	annealed phase				mesophase		
sample	T_{sm} (°C)	T_2 (°C)	ΔH_{sm} (J/g)	ΔH_2 (J/g)	T_{sm1} (°C)	T_{sm2} (°C)	T_2 (°C)
PDT	52	103	60	13	54	67	103
PTT	68	104	64	34	53	64	104
PHT	77	102	53	26	60 (sh)	82	102
POT	84	103	65	32	62 (sh)	85	103

[a] T_{sm} = side chain melt, T_2 = main chain melt, ΔH_{sm} = area under the entire low-temperature region, and ΔH_2 = area under the main chain melting region.

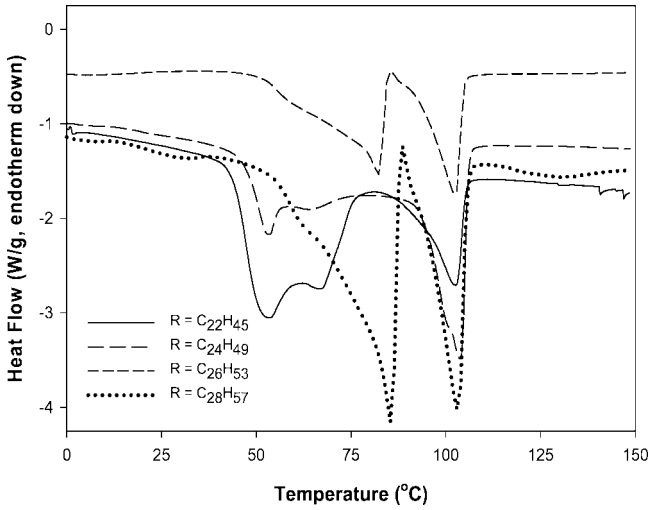

Figure 4. DSC thermograms of regioregular poly(3-alkylthiophene)s containing the mesophase: solid line, **PDT**; long dashes, **PTT**; short dashes, **PHT**; dotted line, **POT**. Scans were run at 10 °C/min under flowing nitrogen gas.

length. All of the DSC determined transition temperatures and peak areas are summarized in Table 3.

Figure 4 shows the DSC thermograms of the samples containing the mesophase, which exhibit significant changes in the endotherm in the side chain melting region. In the presence of the mesophase the endotherm in the region of the side chain melting has a sharp maximum and one or more shoulders. In the main chain melting region of the thermogram there is little difference in the endotherm for the two samples. The complicated nature of the endotherms in the side chain melting region precluded meaningful integrations (the overlap between peaks is too great) so no heats of fusion were measured. The peak maxima temperatures for the mesophases are reported in Table 3.

The unusual sharpness of the peak maxima for the mesophases, especially for **PHT** and **POT**, suggests that there is an exotherm overlapping the observed endotherms. This would imply that that the mesophase, upon heating, has a melting event quickly followed by a crystallization event.

To assist in assigning the phase transitions observed in the DSC thermograms, the temperature dependence of the reflection spectra is used. An example of this is shown in Figure 5 for **POT**. The color change from the violet state to the yellow state matches the high-temperature endotherm. The high-temperature transition is consistent with previous assignments of the thermochromic transition in poly(3-alkylthiophene)s:[10] the high-temperature color change is associated with the main chain melting. As the main chain melts, the polymer backbone loses planarity, which causes a reduction in the extent of conjugation of the π system. This, in turn, causes a blue shift in the electronic absorption, resulting in the yellow color. In contrast, the color change associated with the loss of the mesophase is less well-

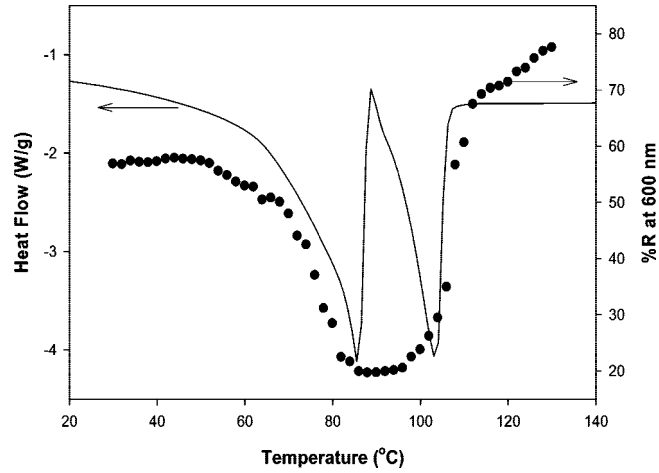

Figure 5. Comparison of the thermogram of **POT** containing mesophase (solid line, left axis) with the temperature dependence of the reflectivity at 600 nm (circles, right axis).

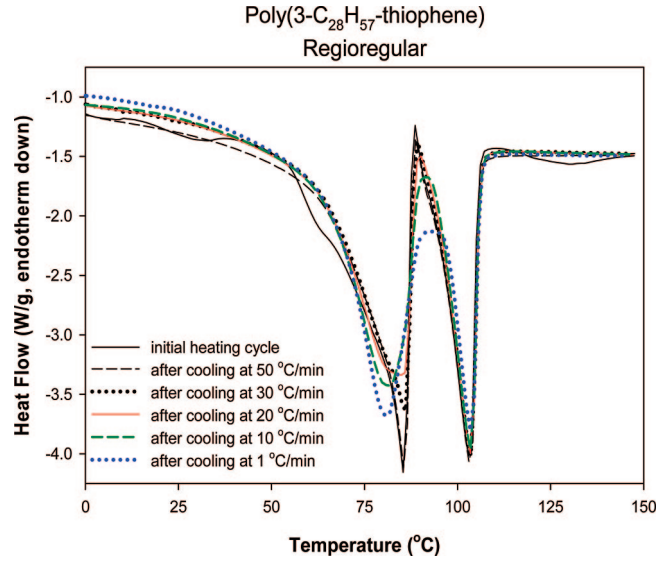

Figure 6. DSC thermograms of **POT** after different cooling rates. The sample was initially prepared containing the mesophase. The heating scans were run at 10 °C/min under flowing nitrogen gas.

defined. The color change from the red state (mesophase) to the violet state is in the region of the sharp peak in the side chain melting region. Examination of the data in Tables 1 and 3 suggests that the electronic change is driven by the hidden crystallization event. The mesophase is blue-shifted relative to the ground state, which implies some loss of conjugation.

To test the kinetics of the evolution of the mesophase, a series of thermograms were recorded after the sample was cooled at different rates. The results of this experiment for **POT** are shown in Figure 6. The sample was initially prepared containing the mesophase, so the characteristic sharp peak (at 85 °C for R = $C_{28}H_{57}$) in the side chain melting region is present. When the sample is cooled at 50 °C/min, the subsequent heating cycle thermogram is identical to the initial measurement, indicating that a cooling rate just less than 1 °C/s is required to freeze out the mesophase. When the cooling rate is reduced to 30 °C/min, the sharp peak at 85 °C in the heating cycle is slightly reduced in intensity. After each cooling cycle, with sequentially smaller cooling rates, the peak of the endotherm in the side chain melting region gradually shifts to lower temperature and broadens. At the slowest cooling rate, 1 °C/min, no evidence of the mesophase exists in the thermogram. In contrast, the high-temperature endotherm is unaffected by the cooling rate.

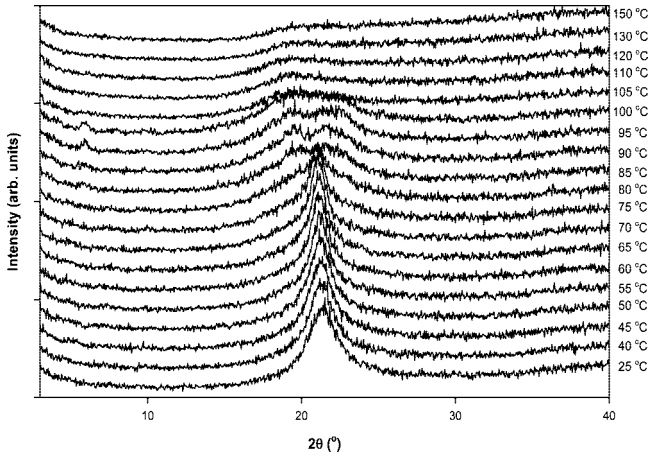

Figure 7. XRD patterns for **RR-PTT** containing the mesophase as the sample is warmed from 25 to 150 °C. Each diffraction pattern is off set from baseline for clarity.

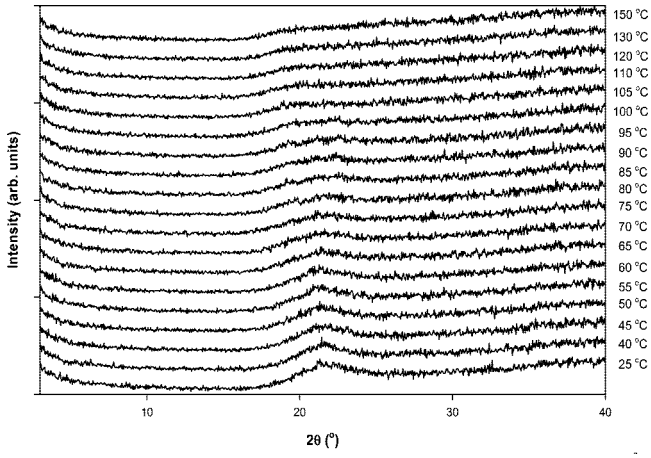

Figure 8. XRD patterns for **PTT** after annealing as the sample is warmed from 25 to 150 °C. Each diffraction pattern is offset from baseline for clarity.

To better understand the structural changes in the different phases, variable temperature XRD measurements were made. Samples were prepared containing the mesophase and the XRD patterns determined during warming. A typical example for **PTT** is shown in Figure 7 (data for the other samples is given in the Supporting Information). All samples showed weak diffraction patterns indicative of low crystallinity. At room temperature there is a single broad peak centered at $2\theta = 21.4°$ ($d = 4.15$ Å). As the sample is warmed, the peak maximum slowly shifts to smaller 2θ and broadens slightly. Between 80 and 85 °C the diffraction pattern dramatically changes, indicative of crystallization occurring: a new peak is observed at $2\theta = 5.8°$ ($d = 15.2$ Å), and the higher angle peak splits into two maxima at $2\theta = 19.8°$ ($d = 4.48$ Å) and $2\theta = 21.7°$ ($d = 4.09$ Å). Upon further warming, between 100 and 105 °C, the low angle peaks disappear; the high angle feature shifts to a single, weak, and broad peak centered at $2\theta = 19.4°$ ($d = 4.57$ Å). The transition at 80 °C is crystallization with loss of the mesophase while the 100 °C transition is to the isotropic melt.

Figure 8 shows the variable temperature XRD pattern of PTT after slowly cooling to room temperature so that the sample is in the annealed phase. The intensity of the diffraction is markedly less than the initial sample, and there is only a single broad peak at $2\theta = 21.4°$ ($d = 4.15$ Å). As the sample is heated, there is a slight shift in the peak maximum near 80 °C and the change to the isotropic melt occurs at 100 °C. The overall low intensity of the diffraction pattern implies that the slow cooling leads to a largely amorphous sample or that the crystallite size is quite small (consistent with the low scattering observed in the reflection spectra), which precludes any observation of peaks in the low angle region. The diffraction pattern for the second heating cycle for the other materials is given in the Supporting Information and shows similar behavior to PTT.

Table 4. Diffraction Maxima and Peak Assignments for the Crystallized Phase between 80 and 100 °C

	hkl					
	200		*h*20		002	
sample	2θ (deg)	*d* (Å)	2θ (deg)	*d* (Å)	2θ (deg)	*d* (Å)
PDT	6.2	14.2	19.7	4.50	21.9	4.06
PTT	5.8	15.2	19.8	4.48	21.7	4.09
PHT	5.6	15.8	19.8	4.48	21.6	4.11
POT	5.2	17.0	19.9	4.46	21.6	4.11

Prosa, Winokur, and McCullough[14] found that two structures can be formed in regioregular poly(3-octylthiophene) and poly(3-dodecylthiophene), which they labeled type I and type II. In the type I structure the polythiophene conjugated chain lies along the crystallographic *c* axis. The chains stack along the *b* axis with a $\pi-\pi$ distance of about 4.5 Å and with alternating location of the S in the thiophene ring. The alkyl chains are tilted away from the plane of the thiophene rings such that, while the alkyl groups are nested, there is minimal overlap or interdigitation between the alkyl groups in the crystallographic *c* direction. The type II structure arises from a small canting of the thiophene chain so the $\pi-\pi$ distance between polythiophene chains increases slightly and the alkyl side chains become interdigitated.

The crystallized phase between 80 and 100 °C in each sample can be assigned to a modified type I structure.[14] The *hkl* assignments for each polymer are given in Table 4. The interplanar spacing, *hkl* = 020, and the chain axis spacing, *hkl* = 002, are relatively constant and similar to the values found for the C_8 and C_{12} analogues reported earlier.[14] The distance between thiophene chains along the *a* axis increases with increasing alkyl chain length (28.4, 30.4, 31.6, and 34.0 Å, respectively, for **PDT**, **PTT**, **PHT**, and **POT**). These distances are short, given the length of the alkyl side chains, which implies that the alkyl chains are disordered, thereby allowing a closer approach of the thiophene chains. The slow cooled samples also are assigned to the type I structure, albeit with low crystallinity. Apparently even slow cooling does not allow development of large crystallites in these PATs.

Rapid cooling from the isotropic melt gives a modestly ordered kinetic phase, consistent with the low intensity of XRD peaks in the low angle region and the minimal scattering in the optical spectra. The XRD data suggest that the mesophase has a structure with interplanar spacings similar to the type I structure but with the side chains only moderately ordered. Upon heating, the interdigitated portions of the alkyl side chains melt (T_{sm1} in the DSC), which allows recrystallization into the type I structure (a similar observation was made for the type II structure for poly(3-octylthiophene) and poly(3-dodecylthiophene)[14]). The sides chains in the type I structure melt (T_{sm2} from the DSC) while the lamellae from the main polymer chains remain intact. Above 100 °C, the isotropic melt occurs (T_2) and only the amorphous halo remains in the diffraction pattern. The optical data support this interpretation. In the mesophase there is a blue shift in the reflection spectrum (the exciton peak absorption is at higher energy), suggesting that the $\pi-\pi$ interaction is weaker and that the thiophene rings are farther apart in the *b* direction. The weaker $\pi-\pi$ coupling also allows fluorescence to be observed. Upon heating, the mesophase anneals to the type I structure, which has stronger $\pi-\pi$ coupling, leading to the red shift in the optical spectrum and the loss of

the emission peak. Finally, at the isotropic melt, the polythiophene chain loses order, twisting sufficiently to lose the $\pi-\pi$ coupling along the *b* axis and to significantly reduce the conjugation along the polymer backbone. This leads to the strong blue shift in the reflection spectrum and the large increase in the luminescence spectrum.

Conclusions

Poly(3-alkylthiophene)s with very long *n*-alkyl substituents (C_nH_{2n+1}, $n = 22$, 24, 26, and 28) were prepared, and the thermochromic properties were investigated. The presence of the long *n*-alkyl side chain allows for the generation of a monotropic mesophase upon rapid cooling. The mesophase is structurally distinct from either the high-temperature phase (an isotropic melt) or the natural low-temperature phase (type I structure). The length of the side chain is inversely related to the rate of cooling required to generate the mesophase.

The poly(3-alkylthiophene) mesophase structure has the alkyl groups only moderately ordered, which increases the spacing between the thiophene chains. This structure reduces the $\pi-\pi$ interaction between the thiophene π systems on adjacent chains, leading to a blue shift in the reflection spectrum and a weak emission in the luminescence spectrum. The DSC thermograms indicate that the mesophase has a small, low-temperature endotherm, possibly associated with melting of lamellae associated with the interdigitated portion of the structure. Once this melt has occurred, the interaction between side chains is reduced and crystallization to the type I structure transpires. The temperature of crystallization to the type I structure is above the side chain melting temperature, so the crystallization is accompanied by a nearly immediate endotherm assigned to melting of the alkyl side chain lamellae. In the type I structure, the thiophene rings are closely spaced so that the nearest-neighbor $\pi-\pi$ interaction is maximized, leading to a red-shifted reflection spectrum and loss of emission. At higher temperature, the DSC, XRD, and spectroscopic measurements all indicate a transition to the isotropic melt between 105 and 110 °C, independent of the length of the alkyl side chain. The high-temperature state has the thiophene rings twisted away from coplanarity, which significantly reduces the π conjugation. The loss of conjugation leads to a strongly blue-shifted optical spectrum and a highly emissive luminescence spectrum.

Acknowledgment. The authors acknowledge KM Scientific, the University of Rhode Island Transportation Center (funded by the U.S. Department of Transportation), the URI Foundation, and the URI Sensors and Surface Technology Partnership for financial support. We also thank Caitlin Macglaflin for assistance in some of the DSC measurements.

Supporting Information Available: XRD diffractograms of all samples in this study. This material is available free of charge via the Internet at http://pubs.acs.org.

References and Notes

(1) Brédas, J.-L., Silbey, R., Eds.; *Conjugated Polymers: The Novel Science of Technology of Highly Conducting and Nonlinear Optically Active Materials*; Kluwer Academic Publishers: Dordecht, 1991.
(2) Salaneck, W. R.; Stafstrom, S.; Brédas, J. L. *Conjugated Polymer Surfaces and Interfaces: Electronic and Chemical Structure of Interfaces for Polymer Light Emitting Devices*; Cambridge University Press: Cambridge, UK, 2003.
(3) Fichou, D., Ed.; *Handbook of Oligo- and Polythiophenes*; Wiley: New York, 1999.
(4) Rughooputh, S. D. D. V.; Hotta, S.; Heeger, A. J.; Wudl, F. *J. Polym. Sci., Part B: Polym. Phys.* **1987**, *25*, 1071–1078.
(5) Roux, C.; Bergeron, J.-Y.; Leclerc, M. *Makromol. Chem.* **1993**, *194*, 869–877.
(6) Roux, C.; Leclerc, M. *Chem. Mater.* **1994**, *6*, 620–624.
(7) Faïd, K.; Fréchette, M.; Ranger, M.; Mazerolle, L.; Lévesque, I.; Leclerc, M.; Chen, T.-A.; Rieke, R. D. *Chem. Mater.* **1995**, *7*, 1390–1396.
(8) DiCésare, N.; Belletête, M.; Leclerc, M.; Durocher, G. *Chem. Phys. Lett.* **1998**, *291*, 487–495.
(9) Garreau, S.; Leclerc, M.; Errien, N.; Louarn, G. *Macromolecules* **2003**, *36*, 692–697.
(10) Yang, C.; Orfino, F. P.; Holdcroft, S. *Macromolecules* **1996**, *29*, 6510–6517.
(11) Yang, C.; Holdcroft, S. *Synth. Met.* **1997**, *84*, 563–564.
(12) Hsu, W.-P.; Kevon, K.; Ho, K.-S.; Myerson, A. S.; Kwei, T. K. *Macromolecules* **1993**, *26*, 1318–1323.
(13) Park, K. C.; Levon, K. *Macromolecules* **1997**, *30*, 3175–3183.
(14) Prosa, T. J.; Winokur, M. J.; McCullough, R. D. *Macromolecules* **1996**, *29*, 3654–3656.
(15) Bolognesi, A.; Porzio, W.; Provasoli, F.; Ezquerra, T. *Makromol. Chem.* **1993**, *194*, 817–827.
(16) Wang, Y.; Archambault, N.; Marold, A.; Weng, L.; Lucht, B. L.; Euler, W. B. *Macromolecules* **2004**, *37*, 5415–5422.
(17) Wang, Y.; Euler, W. B.; Lucht, B. L. *Chem. Commun.* **2004**, 686–687.
(18) Wang, Y.; Mills, A.; Euler, W. B.; Lucht, B. L. *Chem. Commun.* **2006**, 2121–2122.
(19) Leclerc, M.; Diaz, F. M.; Wegner, G. *Makromol. Chem.* **1989**, *190*, 3105–3116.
(20) Loewe, R. S.; Khersonsky, S. M.; McCullough, R. D. *Adv. Mater.* **1999**, *11*, 250–253.
(21) The molecular weight for the regioregular and regoirregular poly(3-docosylthiophene) were reversed in Table 1 of ref 16.
(22) Tachibana, T.; Hosaka, N.; Tokura, Y. *Macromolecules* **2001**, *34*, 1823–1827.
(23) Yamamoto, T.; Komarudin, D.; Arai, M.; Lee, B.-L.; Suganuma, H.; Asakawa, N.; Inoue, Y.; Kuboto, K.; Sasaki, S.; Fukuda, T.; Matsuda, H. *J. Am. Chem. Soc.* **1998**, *120*, 2047–2058.

MA801352F